Article

J. Mex. Chem. Soc. **2016**, *60(2)*, 62-66

ISSN 1870-249X

Antibacterial Activity of Pipemidic Acid ions-MgFeAl Layered Double Hydroxide Hybrid Against *E. coli* and *S. typhi*

Alejandra Santana-Cruz,[1] Jorge Luis Flores-Moreno,[*,1] Roberto Guerra-González[2] and María de Jesús Martínez-Ortiz[3]

[1] Departamento de Ciencias Básicas, Universidad Autónoma Metropolitana-Azcapotzalco. Av. San Pablo 180, Col. Reynosa Tamaulipas, C.P. 02200, México D.F., México.
[2] Universidad Michoacana de San Nicolás de Hidalgo, Facultad de Ingeniería Química, Avenida Francisco J. Múgica s/n Ciudad Universitaria. C.P. 58030, Morelia, Michoacán, México.
[3] Instituto Politécnico Nacional, ESIQIE, Avenida IPN UPALM Edificio 7, Zacatenco, 07738 México D.F., México.
* Corresponding author: Departamento de Ciencias Básicas, Universidad Autónoma Metropolitana-Azcapotzalco. Av. San Pablo 180, Col. Reynosa Tamaulipas, C.P. 02200, México D.F.
email: jflores@correo.azc.uam.mx, Tel: +52 55-53189000 ext. 2233.

Received January 15th, 2016; Accepted April 4th, 2016.

Abstract. An anion exchange process was used to prepare pipemidic acid-MgFeAl composite from MgFeAl-Cl layered double hydroxide as inorganic matrix. The obtained hybrid material contains pipemidic acid anions as well as, in a less extent; carbonate and chloride species in its interlayer space. The antibacterial properties were evaluated against *E. coli* and *S. typhi* strains through dilution broth method. MgFeAl-Cl matrix resulted to be completely inactive against two bacteria, while MgFeAl-PIP composite killed all colonies of *E. coli* after 90 min of exposure and showed a good activity to kill *S. typhi* bacteria at times as short as 120 min.
Key words: layered double hydroxide; pipemidic acid; hybrid material; intercalation; antibacterial activity.

Resumen. Se preparó el material híbrido ácido pipemídico-MgFeAl por intercambio iónico partiendo del hidróxido doble laminar MgFeAl-Cl, usado como matriz inorgánica receptora. El material híbrido obtenido contiene en su región interlaminar aniones del ácido pipemídico, así como también, en menor medida; iones carbonato y cloruro que no fueron intercambiados. Las propiedades antibacteriales contra cepas de *E. coli* y *S. typhi* fueron evaluadas mediante el método de dilución en caldo. La matriz inorgánica de partida MgFeAl-Cl no presentó actividad antibacterial alguna; sin embargo, el material híbrido MgFeAl-PIP eliminó la totalidad de las colonias de *E. coli* luego de 90 min de exposición y presentó buena actividad contra bacterias de *S. typhi* después de 120 min.
Palabras clave: hidróxido doble laminar; ácido pipemídico; material híbrido; intercalación; actividad antibacterial.

Introduction

The synthesis of hybrid inorganic-organic systems for human health has received considerable attention. The interest focuses on the synergistic properties, effects and new potential uses. In particular, hybrid materials prepared by intercalation of bioactive molecules into the galleries of layered double hydroxides (LDHs) result in a wide spectrum of versatile materials [1,2]. The application field of these composites depends on the nature of the intercalated anion, thus different LDHs have been used as guests for nonsteroidal anti-inflammatory drugs [3,4], sunscreen agents [5-7], molecules with antioxidant properties [8,9], anticancer drugs [10-12], antibiotics [13-16], and even for DNA and genes [17-19]. In this sense, many efforts have been made aiming to protect the bioactive molecules from degradation, or to enhance the bioavailability and release properties.

Layered double hydroxides belong to a family of interesting inorganic matrices, represented by the general formula $\left[M^{2+}_{1-x}M^{3+}_{x}\left(OH\right)_2\right]A^{n-}_{x/n}\cdot mH_2O$, where M^{2+} and M^{3+} are cations, and A represents either inorganic or organic anions [20,21]. The LDH structure is based on $Mg(OH)_6$ octahedral units sharing edges in order to form $Mg(OH)_2$ brucite-like layers. The octahedral units may contain either divalent (Mg^{2+}, Ni^{2+}, Zn^{2+}, Cu^{2+}, Co^{2+}, etc.) or trivalent cations (Al^{3+}, Fe^{3+}, Ga^{3+}, Cr^{3+}, etc.) resulting in positively charged sheets. Electroneutrality of the system requires the presence of anions and water molecules occupying the interlayer region, leading to the stacking of the double hydroxide layers.

Pipemidic acid (PA), 8-Ethyl-5-oxo-2-piperazin-1-yl-5,8-dihydropyrido[2,3-d]pyrimidine-6-carboxylic acid (Scheme 1), is a derivative of piromidic acid. It is active against gram-negative bacteria as well as some gram-positive bacteria, but it is active against resistant bacteria to piromidic acid and nalidixic acid.

This work deals with synthesis of a hybrid material through the intercalation of pipemidic acid anions into galleries of MgFeAl LDH. The aim was to study their properties as antibacterial agent against *E. coli* and *S. typhi* strains.

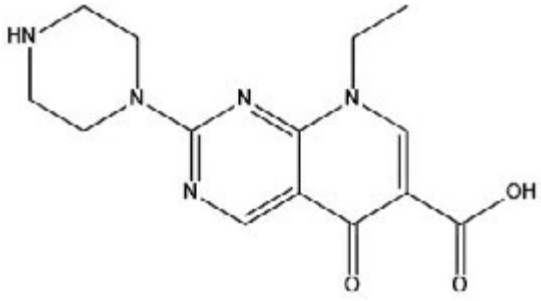

Scheme 1. Chemical structure of pipemidic acid.

Experimental

Sample Preparation

The pristine MgFeAl-CO_3, containing carbonate ions in the interlayer region, was synthetized by conventional coprecipitation method under high supersaturation conditions [22]. A 1M Mg^{2+}, Al^{3+}, and Fe^{3+} solution was prepared by dissolving the corresponding nitrates salts in deionized water. The following molar ratios were used, $Mg^{2+}/(Fe^{3+} + Al^{3+}) = 3$, $Al^{3+}/Fe^{3+} = 3.6$. Separately, a 1M aqueous solution containing Na_2CO_3 and KOH was prepared. The alkaline solution was added dropwise under vigorous stirring to the metallic solution until pH = 9 was reached. The resulting suspension was then aged at 80 °C for 16 h. At the end of aging, the solid was centrifuged and washed several times with deionized water. Finally, the solid was dried overnight at 120 °C in an oven yielding the sample named MgFeAl-CO_3.

The MgFeAl-Cl LDH was prepared by suspending the MgFeAl-CO_3 sample in a 0.1 M solution of NaCl. The above suspension was then titrated with HCl 0.1 M at pH = 5. The resulting solid was centrifuged and washed several times with CO_2-free deionized water. The dried solid was stored under vacuum before using.

The intercalated MgFeAl-PIP sample (PIP are pipemidic acid anions) was synthetized by an anion exchange reaction [23]. Pipemidic acid is nearly insoluble in water, thus, to generate a soluble sodium salt, a suspension of pipemidic acid (2.8 mmol in 25 mL of CO_2-free deionized water) was reacted with the stoichiometric amount of NaOH and the final pH was adjusted to 9. The resulting solution was bubbled with argon before adding MgFeAl-Cl LDH (molar ratio PIP/M^{3+} = 2). The bubbling was maintained for 1 h. Then, the system was sealed under argon. After seven days of stirring, the MgFeAl-PIP was then separated by centrifugation, washed several times with warm CO_2-free deionized water, dried at 80 °C overnight and finally stored under vacuum.

Antibacterial activity

The *Escherichia coli* ATCC® 14028 and *Salmonella typhi* ATCC® 25922 strains were supplied from the Laboratorio Estatal de Salud Pública de Michoacán. The antibacterial activity of the pristine MgFeAl-Cl LDH and the MgFeAl-PIP composite, against both pathogenic bacteria, was evaluated by agar well diffusion method, according to the procedure previously reported [24-26]. The Minimum Inhibitory Concentration (MIC), defined as the lowest concentration of a particular antibiotic where the absence of visible growth is recorded, was also determined on plates of agar dilution and broth dilution assays. Similar techniques were used to determine the Minimum Bactericidal Concentration (MBC). The MBC is defined as the lowest concentration of an antibacterial agent needed to kill a particular bacterium. Both, agar dilution and broth dilution assays provided similar MIC and MBC values. Both cultures were grown and maintained in tripticaseine broth medium. A starter culture of each strain was inoculated with fresh colonies and then incubated for 24 h in tripticaseine medium, the inoculum consisted of 10^9 bacteria/mL. Fresh medium was inoculated in tests tubes with the starter culture and grown at 35.5 °C under continuous stirring at 30 rpm. MgFeAl-Cl or MgFeAl-PIP were added to bacterial cultures at an average MBC, previously determined for each material. Then, samples were taken at different intervals of time and seeded in Petri dishes previously loaded with 30 mL of selective agar. Finally, the dishes were incubated at 35.5 °C under aerobic conditions and the number of surviving colonies was determined. As a control, a plate was inoculated without bactericide material. All the materials were sterilized during experiments with bacteria.

Characterization

Powder X-ray diffraction (PXRD) patterns were recorded using $CuK_{\alpha 1}$ (λ = 1.5406 Å) on a Philips X'Pert instrument operating at 45 kV and 45 mA in the 2θ range of 4-80°.

Infrared spectra were recorded in the range of 4000-400 cm^{-1} using an FTIR Nicolet Magna IR 750 infrared spectrometer. Samples were diluted with KBr and then pressed to form discs.

Results and discussion

PXRD patterns of MgFeAl-Cl LDH and MgFeAl-PIP composite are given in Fig. 1 and the unit cell *c* parameters are shown in Table 1.

Table 1. The unit cell *c* parameters obtained for pristine MgFeAl-Cl LDH and MgFeAl-PIP composite.

Sample	MgFeAl-Cl	MgFeAl-PIP
d_{003} (Å)	7.80	14.13
d_{006} (Å)	3.92	7.04
Lattice parameter c^a (Å)	23.40	42.39

[a] The unit cell *c* parameter was calculated according to $c = 3d_{003}$

The XRD reflections of the pristine MgFeAl-Cl LDH are attributed to hydrotalcite structure (JCPDS 22-700) and confirm the formation of a layered structure with a basal spacing of 7.80 Å. This value agrees well with those reported for MgFeAl-Cl LDH with similar composition [27,28]. Thus, the sharp peak at 2θ = 11.33° corresponds to the (*003*) plane of the hexagonal structure with rhombohedral symmetry. The position of the (*003*) reflection depends on the number, orientation and nature of anions hosted in the interlayer region. The (*003*) peak for the MgFeAl-PIP composite is observed at 2θ = 6.25° (14.13 Å). The increase of the interlayer distance from 7.80 to 14.13 Å indicates the effective intercalation of the PIP anions. Thus, as a result of the increase in the basal spacing after exchange, the lattice structure of LDH expanded to the c-axis direction. As the brucite-like layer thickness is 4.8 Å [29], the gallery height can be estimated to be 9.33 Å for MgFeAl-PIP. This gallery height seems to be small to allow hosting such a big anion molecule. Such dimension can be only explained assuming that the intercalated anions molecules are arranged in a monolayer with a tilted orientation toward the brucite-like sheets. Nevertheless, the peaks observed near to 2θ = 11.33°, and 22.89° (Fig. 1b) indicate that the exchange of chloride anions by pipemidic acid anions was incomplete. Additionally, the small peak at 2θ = 9.75° might be due to intercalation of some pipemidic acid anions with the main axis oriented parallel to the layers of the LDH. It is worth mentioning that none reflection attributable to the pipemidic acid sodium salt was observed. In fact, XRD analysis of the pipemidic acid sodium salt (not included) showed the presence of a completely amorphous phase. However, as Fig. 1b indicates, XRD pattern of the MgFeAl-PIP hybrid material is not a combination of the XRD patterns of the pristine MgFeAl-Cl LDH and the pipemidic acid sodium salt, which indicates that, indeed, the intercalation of the pipemidic acid anions was successful.

The FTIR spectra for MgFeAl-Cl LDH and MgFeAl-PIP composite are shown in Fig. 2. It is known that pipemidc acid do not show a υ(C=O) absorption because the carboxylic group is deprotonated and the molecule exists as a zwitterion [30,31]. Instead, two characteristic bands in the range of 1650-1510 cm^{-1} and 1400-1280 cm^{-1} are typical for similar ionic carboxylates[32]. These bands are attributable to asymmetrical and symmetrical stretching vibrations of COO^- group, respectively. The FTIR spectrum (not shown) of the pipemidic acid shows two strong bands at 1640 and 1618 cm^{-1} which are assigned to the carbonyl ring group and to the asymmetrical stretching vibrations of COO^- group, respectively. The pipemidic acid sodium salt (for clarity not shown) shows a very similar FTIR spectrum to that of pipemidic acid, confirming that the band at 1640 cm^{-1} (1633 cm^{-1} for the sodium salt) belongs to the stretching vibrations of COO^- group.

For both MgFeAl-Cl LDH (Fig. 2a) and MgFeAl-PIP composite (Fig. 2b), the broad absorption band around 3500 cm^{-1} is due to O-H stretching vibration of the hydroxyl groups conforming the brucite-like layers and water in the interlaminar region. The O-H bending vibration of the interlayer water is observed at 1637 cm^{-1}. Besides, MgFeAl-Cl LDH exhibits two bands situated at 1384 and 1364 cm^{-1} which can be ascribed to υ_3 modes of the carbonate ion.

This indicates that a scarce amount of CO_3^{2-} ions remained in the interlayer region after anion exchange process; nevertheless, none reflection ascribed to the intercalation of CO_3^{2-} ions could be observed by XRD. In fact, according to some reports, MgAl-CO_3 layered double hydroxide exhibits a broad band centered at about 1364 cm^{-1} assigned to interlayered carbonate anions. After deconvolution, these band decomposes in two components situated a 1388 and 1364 cm^{-1}, attributed to υ_3-CO_3^{2-} modes. The presence of a single band or a two-split band depends on the symmetry of the CO_3^{2-} ion [33-35].

As a consequence of the antibiotic molecule intercalation, the MgFeAl-PIP composite shows a rather complex FTIR spectrum composed by a combination of IR bands belonging to the layered phase and to the antibiotic molecule. The band at

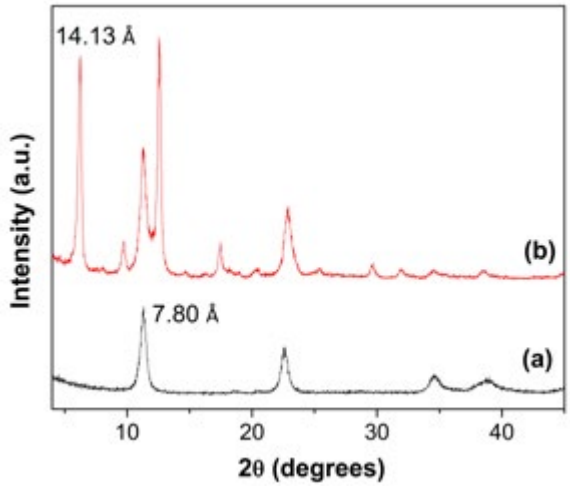

Fig. 1. Powder X-ray diffraction of (a) MgFeAl-Cl LDH and (b) MgFeAl-PIP composite.

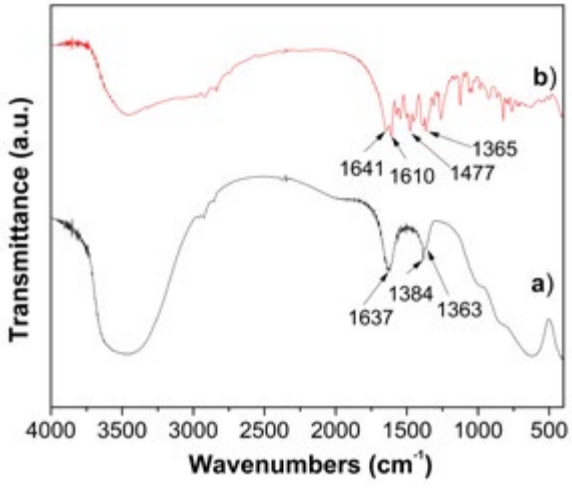

Fig. 2. FTIR spectra of (a) MgFeAl-Cl LDH and (b) MgFeAl-PIP composite.

1641 cm^{-1} is ascribed to the carbonyl ring group, while the band at 1610 cm^{-1} belongs to the asymmetrical stretching vibrations of COO^- group.

Results from both, XRD and FTIR analysis, confirm the intercalation of the antibiotic molecule into the galleries of the MgFeAl-LDH.

The MIC and the MBC values are reported in Table 2. The results indicate that MgFeAl-PIP hybrid material is slightly more effective against *E. coli* than *S. typhi*. The MgFeAl-Cl and MgFeAl-NO_3 (included as a reference) did not show antimicrobial activity. As a comparison, the MIC of pure pipemidic acid were found to be 1.56 µg/mL and 3.13 µg/mL against *E. coli* and *S. typhi*, respectively, suggesting that PA is, in fact, twice more active for *E. coli* than *S. typhi* [36].

Table 2. The MIC and the MBC values of layered and composite materials against *E. coli* (Gram negative) and *S. typhi* (Gram negative) bacteria.

Material	MIC (mg/mL)[a,b]		MBC (mg/mL)[a,b]	
	E. coli	S. typhi	E. coli	S. typhi
MgFeAl-CO_3	N.A.	N.A.	N.A.	N.A.
MgFeAl-NO_3	N.A.	N.A.	N.A.	N.A.
MgFeAl-Cl	N.A.	N.A.	N.A.	N.A.
MgFeAl-PIP	3.5	4.5	4.0	5.0

[a] N.A. No Activity, [b] on the basis of the mass of material.

In order to study the kinetics of the antimicrobial action of MgFeAl-LDHs (as reference) and MgFeAl-PIP composite a time-kill test at concentrations corresponding to the MBC value (Table 2) was achieved. As shown in (Fig. 3), *E. coli* bacteria multiply rapidly with time in presence of carbonate and nitrate containing MgFeAl-LDH, the number of colonies duplicated after 20 and 93 min, respectively, confirming null antimicrobial activity. As to MgFeAl-Cl LDH, it behaves almost as a bacteriostatic material during time. In this regard, it has been proven that other common LDHs such as ZnAl-CO_3 [37,38], MgAl-CO_3 and MgAl-NO_3 [39] do not exhibit any antibacterial activity against *E. coli*. Same conclusion was established for MgAl-NO_3 against *S. aureus* [40]. This demonstrates that LDHs do not exhibit any antibacterial characteristic by themselves, even if they contain chloride anions in their interlayer region. Finally, based on the results in Fig. 3, it is clear that the effect of the inorganic compensating anion (CO_3^{2-}, NO_3^- or Cl^-) on the growth rate is quite different. In contrast, the MgFeAl-PIP hybrid material showed a total fungicidal effect and none bacteria remain alive after 30 min. It seems noticeable that antibacterial properties of the pipemidic acid molecule were preserved after intercalation into the LDH. Thus, the hybrid material resulted in an efficient antibacterial system against *E. coli*.

On the other hand, Fig. 4 shows results of kinetics of antibacterial tests for MgFeAl-LDHs and MgFeAl-PIP composite against *S. typhi*. As observed for *E. coli* in Fig. 3, none of the inorganic anion containing LDHs showed antibacterial action.

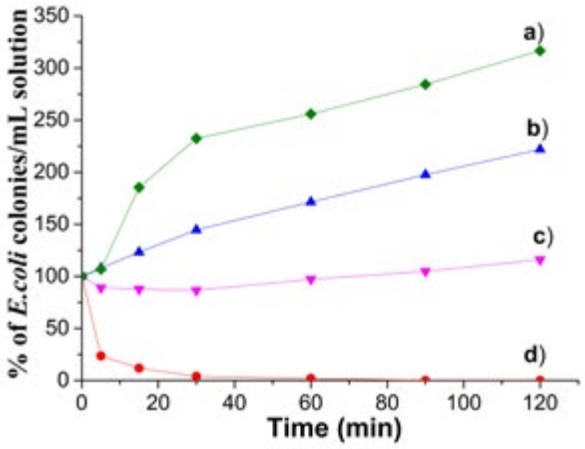

Fig. 3. Percentage of *E. coli* colonies surviving in culture media in presence of a) MgFeAl-CO_3 LDH, b) MgFeAl-NO_3 LDH c)MgFeAl-Cl LDH and d) MgFeAl-PIP hybrid material. Each material was evaluated at MBC.

In this case, MgFeAl-Cl allows rapid development of colonies of *S. typhi*. Conversely, MgFeAl-PIP hybrid material showed good activity to eliminate bacteria, as only 12% of colonies survived after 90 min of exposure. As previously pointed out by results of MIC and MBC values, MgFeAl-PIP is less active to eliminate *S. typhi* than *E. coli* pathogens. These results are in good agreement with the data previously reported for the antibacterial activity of supported gold nanoparticles against *E. coli* and *S. typhi* [24]. Independently of the bactericide material, it is harder to kill *S. typhi* than *E. coli* because the first one has a very complex and resistant plasmatic membrane [41].

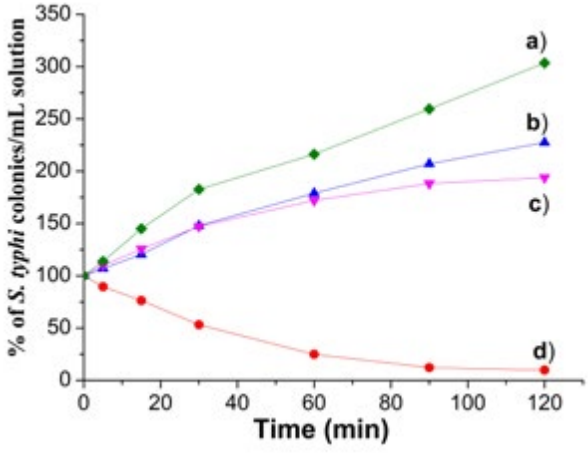

Fig. 4. Percentage of *S. typhi* colonies surviving in culture media in presence of a) MgFeAl-CO_3 LDH, b) MgFeAl-NO_3 LDH c) MgFeAl-Cl LDH and d) MgFeAl-PIP hybrid material. Each material was evaluated at MBC.

Conclusions

MgFeAl-PIP composite was prepared by exchanging pipemidic acid anions into the interlayer space of MgFeAl-Cl LDH. The exchange degree was not complete, as some Cl^- anions remained in the interlayer space. The gallery height estimated to be 9.33 Å suggested that pipemidic acid anions were intercalated as a monolayer in a tilted mode. However, some molecules were probably intercalated parallel to brucite-like sheets. MgFeAl-PIP hybrid showed efficient antibacterial activity against *E. coli* and *S. typhi*. The pristine MgFeAl LDH chosen in this work resulted to be a very good biocompatible inorganic host, as it cares not killing bacteria by itself, but it allows driving the release of biologically active molecules into the media growth with time. MgFeAl-PIP composite eliminated all colonies of *E. coli* after 90 min of exposure and showed good activity to eliminate *S. typhi* bacteria at times as short as 120 min.

Acknowledgements

ASC gratefully wishes to acknowledge CONACyT for financial support through a Master fellowship.

References

1. Costantino, U.; Nocchetti, M.; Sisani, M.; and Vivani, R. *Zeitschrift für Krist.* **2009**, *224*, 273-281.
2. Del Hoyo, C. *Appl. Clay Sci.* **2007**, *36*, 103-121.
3. Ambrogi, V.; Fardella, G.; Grandolini, G.; and Perioli, L. *Int. J. Pharm.* **2001**, *220*, 23-32.
4. Del Arco, M.; Fernández, A.; Martin, C.; and Rives, V. *Appl. Clay Sci.* **2007**, *36*, 133-140.
5. Perioli, L.; Ambrogi, V.; Bertini, B.; Ricci, M.; Nocchetti, M.; Latterini, L.; and Rossi, C. *Eur. J. Pharm. Biopharm.* **2006**, *62*, 185-193.
6. Perioli, L.; Ambrogi, V.; Rossi, C.; Latterini, L.; Nocchetti, M.; and Costantino, U. *J. Phys. Chem. Solids* **2006**, *67*, 1079-1083.
7. Perioli, L.; Nocchetti, M.; Ambrogi, V.; Latterini, L.; Rossi, C.; and Costantino, U. *Microporous Mesoporous Mater.* **2008**, *107*, 180-189.
8. Lima, E.; Flores, J.; Cruz, A. S.; Leyva-Gómez, G.; and Krötzsch, E. *Microporous Mesoporous Mater.* **2013**, *181*, 1-7.
9. Rossi, C.; Schoubben, A.; Ricci, M.; Perioli, L.; Ambrogi, V.; Latterini, L.; Aloisi, G. G.; and Rossi, A. *Int. J. Pharm.* **2005**, *295*, 47-55.
10. Tyner, K. M.; Schiffman, S. R.; and Giannelis, E. P. *J. Control. Release* **2004**, *95*, 501-514.
11. Pang, X.; Ma, X.; Li, D.; and Hou, W. *Solid State Sci.* **2013**, *16*, 71-75.
12. Chakraborty, M.; Dasgupta, S.; Sengupta, S.; Chakraborty, J.; Ghosh, S.; Ghosh, J.; Mitra, M. K.; Mishra, A.; Mandal, T. K.; and Basu, D. *Ceram. Int.* **2012**, *38*, 941-949.
13. Ryu, S.-J.; Jung, H.; Oh, J.-M.; Lee, J.-K.; and Choy, J.-H. *J. Phys. Chem. Solids* **2010**, *71*, 685-688.
14. San Román, M. S.; Holgado, M. J.; Salinas, B.; and Rives, V. *Appl. Clay Sci.* **2012**, *55*, 158-163.
15. Wang, J.; Liu, Q.; Zhang, G.; Li, Z.; Yang, P.; Jing, X.; Zhang, M.; Liu, T.; and Jiang, Z. *Solid State Sci.* **2009**, *11*, 1597-1601.
16. Trikeriotis, M.; and Ghanotakis, D. F. *Int. J. Pharm.* **2007**, *332*, 176-184.
17. Choy, J.; Kwak, S.; Jeong, Y.; and Park, J. *Angew. Chem. Int. Ed. Engl.* **2000**, *39*, 4041-4045.
18. Choy, J.-H.; Kwak, S.-Y.; Park, J.-S.; Jeong, Y.-J.; and Portier, J. *J. Am. Chem. Soc.* **1999**, *121*, 1399-1400.
19. Choy, J.-H.; Park, J.-S.; Kwak, S.-Y.; Jeong, Y.-J.; and Han, Y.-S. *Mol. Cryst. Liq. Cryst. Sci. Technol. Sect. A. Mol. Cryst. Liq. Cryst.* **2000**, *341*, 425-429.
20. Evans, D. G.; and Slade, R. C. T. In *Layered Double Hydroxides*; Duan, X.; and D. G. Evans, Eds.; Springer Berlin Heidelberg, 2006; pp. 1-87.
21. Cavani, F.; Trifirò, F.; and Vaccari, A. *Catal. Today* **1991**, *11*, 173-301.
22. Auer, S.; Grunwaldt, J.; Köppel, R.; and Baiker, A. *J. Mol. Catal. A Chem.* **1999**, *139*, 305-313.
23. Miyata, S. *Clays Clay Miner.* **1983**, *31*, 305-311.
24. Guerra, R.; Lima, E.; and Guzmán, A. *Microporous Mesoporous Mater.* **2013**, *170*, pp. 62-66.
25. Guerra, R.; Lima, E.; Viniegra, M.; Guzmán, A.; and Lara, V. *Microporous Mesoporous Mater.* **2012**, *147*, 267-273.
26. Lima, E.; Guerra, R.; Lara, V.; and Guzmán, A. *Chem. Cent. J.* **2013**, *7*, 11.
27. Li, S.-P.; Hou, W.-G.; Han, S.-H.; Li, L.-F.; and Zhao, W.-A. *J. Colloid Interface Sci.* **2003**, *257*, 244-249.
28. Del Arco, M.; Fernández, A.; Martin, C.; and Rives, V. *Appl. Clay Sci.* **2009**, *42*, 538-544.
29. Miyata, S. *Clays Clay Miner.* **1975**, *23*, 369-375.
30. Fonseca, I.; Martínez-Carrera, S.; and García-Blanco, S. *Acta Crystallogr. Sect. C Cryst. Struct. Commun.* **1986**, *42*, 1618-1621.
31. Skrzypek, D.; Szymanska, B.; Kovala-Demertzi, D.; Wiecek, J.; Talik, E.; and Demertzis, M. A. *J. Phys. Chem. Solids* **2006**, *67*, 2550-2558.
32. Turel, I. *Coord. Chem. Rev.* **2002**, *232*, 27-47.
33. Tanaka, T.; Kameshima, Y.; Nishimoto, S.; and Miyake, M. *Anal. Methods* **2012**, *4*, 3925.
34. Kloprogge, J. T.; Krisof, J.; and Frost, R. L. In *12th International Clay Conference*; Dominguez, E., Mas, G., & Cravero, F.; Bahai-Blanca, Argentina, 2001.
35. Kloprogge, J. T.; and Frost, R. L. *J. Solid State Chem.* **1999**, *146*, 506-515.
36. Shimizu, M.; Takase, Y.; Nakamura, S.; Katae, H.; and Minami, A. *Antimicrob. Agents Chemother.* **1975**, *8*, 132-138.
37. Mishra, G.; Dash, B.; Pandey, S.; and Mohanty, P. P. *J. Environ. Chem. Eng.* **2013**, *1*, 1124-1130.
38. Ballarin, B.; Mignani, A.; Mogavero, F.; Gabbanini, S.; and Morigi, M. *Appl. Clay Sci.* **2015**, *114*, 303-308.
39. Wang, M.; Hu, Q.; Liang, D.; Li, Y.; Li, S.; Zhang, X.; Xi, M.; and Yang, X. *Appl. Clay Sci.* **2013**, *83-84*, 182-190.
40. Ryu, S.-J.; Jung, H.; Oh, J.-M.; Lee, J.-K.; and Choy, J.-H. *J. Phys. Chem. Solids* **2010**, *71*, 685-688.
41. Atlas, R. M. *Principles of Microbiology*; Editorial Mosby: USA, 1995. pp. 43-55.